ANTICANCER RESEARCH *41*: 5179-5188 (2021)
doi:10.21873/anticanres.15336

Clinical Significance of ^{18}F-fluorodeoxyglucose and Glucose Transporter 1 mRNA in Clear Cell Renal Cell Carcinoma

HIRONORI BETSUNOH[1], SETSU SAKAMOTO[2,3], YASUSHI KAJI[4], AKINORI NUKUI[5], MINORU KOBAYASHI[6], MASAHIRO YASHI[1], KEITARO HAYASHI[7], NAOHIKO ANZAI[8] and TAKAO KAMAI[1]

[1]*Department of Urology, Dokkyo Medical University, Mibu, Japan;*
[2]*Positron Emission Tomography Center, Dokkyo Medical University, Mibu, Japan;*
[3]*Department of Radiology, Hyogo Cancer Center, Akashi, Japan;*
[4]*Department of Radiology, School of Medicine, Dokkyo Medical University, Mibu, Japan;*
[5]*Department of Urology, Tochigi Cancer Center, Utsunomiya, Japan;*
[6]*Department of Urology, Utsunomiya Memorial Hospital, Utsunomiya, Japan;*
[7]*Department of Pharmacology and Toxicology, School of Medicine, Dokkyo Medical University, Mibu, Japan;*
[8]*Department of Pharmacology, Chiba University Graduate School of Medicine, Chiba, Japan*

Abstract. *Background/Aim: ^{18}F-fluorodeoxyglucose (FDG) uptake measurement on positron emission tomography/computed tomography (PET/CT) is difficult in renal tumors because of the nearby renal parenchyma and urinary tract, which excrete FDG. We carefully examined the maximum standardized uptake value (SUV_{max}) on FDG-PET/CT and investigated the relationship between major glucose transporters in the kidney and clear cell renal cell carcinoma (ccRCC) progression. Patients and Methods: Forty-five patients with ccRCC underwent FDG-PET/CT for staging and nephrectomy. Glucose transporter mRNA expression was examined in the removed kidney. Results: SUV_{max} was increased in high-stage and high-grade tumors. Glucose transporter 1 (GLUT1) mRNA expression was higher in tumor tissues, in contrast to other glucose transporters. SUV_{max} was not correlated with GLUT1 mRNA expression. Kaplan-Meier analysis showed reduced overall and recurrence-free survival in the high SUV_{max} group. Conclusion: Primary ccRCC lesions show a high SUV_{max} and GLUT1 mRNA over-expression. SUV_{max} increases with tumor upstaging and upgrading.*

The glucose transport system is located at the cell membrane and found throughout the body but particularly in the kidney and intestine. There are two glucose transporters: the glucose transporter (GLUTs) with 14 members (1) and the sodium-glucose transporter (SGLTs) with 5 members (2). GLUTs and SGLTs act as facilitative and secondary active transport systems, respectively. In this process, glucose is initially transported from the renal tubular lumen to tubular cells by SGLT1 and SGLT2 at the apical membrane, followed by transport to the intravascular lumen by GLUT1 and GLUT2 at the basolateral membrane. Because SGLT2 is a key molecular factor for glucose reabsorption in the kidney, it has recently attracted attention for the development of antidiabetic agents. Several studies have measured SGLT1, GLUT1, or GLUT2 in many malignancies (3-6). Nakajo *et al.* (5) reported that the staining scores of GLUT1 were higher in a high-risk thymic epithelial tumor group than in a low-risk group and identified a significant correlation between ^{18}F-fluorodeoxyglucose (FDG) uptake and GLUT1 staining score. For renal cell carcinomas (RCCs), Chan *et al.* (3) reported that, of GLUT1, GLUT2, GLUT3, and GLUT4, GLUT1 mRNAs were over-expressed. Kobayashi *et al.* (6) investigated GLUT1 and -2 and SGLT1 and -2 expression by immunostaining and determined that they had no significant correlation with pathological variables. FDG-positron emission tomography (PET) is useful for evaluating malignancies and monitoring treatment effect because PET detects the altered glycometabolism of malignancies (3, 5, 7-10). Although some studies have focused on the use of FDG-PET for detecting metastatic RCCs (7, 8), there are few reports on its use in primary RCC (9, 10). One reason for this scant evidence is the close proximity between primary RCC and the urinary tract, which is the site of FDG excretion. Accordingly, care must be taken to not mistake the excreted FDG as a primary RCC lesion.

Correspondence to: Hironori Betsunoh, Department of Urology, Dokkyo Medical University, 880 Kitakobayashi, Mibu, Shimotsuga, Tochigi 321-0293, Japan. Tel: +81 282862162, Fax: +81 282867533, e-mail: hirobets@dokkyomed.ac.jp

Key Words: Renal cell carcinoma, positron emission tomography, glucose transporter 1, maximum standardized uptake value.

In another study, Saito *et al*. (11) analyzed C-reactive protein (CRP) kinetics and overall survival in metastatic RCC and revealed that CRP could be used as a biomarker. However, there was no consideration of whether the prognosis of primary RCC was associated with glycometabolism and CRP. Thus, examination of all factors together could be more important for the prognosis of RCC. In relation to this, glucose transporters (6) and FDG uptake (9) have been studied independently in ccRCC. Accordingly, here, we carefully measured the SUV_{max} of FDG and the mRNA levels of glucose transporters in primary ccRCC lesions to determine whether a high SUV_{max} and over-expression of these mRNAs correlate with tumor progression as the primary endpoint. The secondary endpoint was the relationship of the SUV_{max}, GLUT1 mRNA, and CRP with prognosis.

Patients and Methods

Patients. We retrospectively studied 45 consecutive Japanese patients with ccRCC diagnosed by nephrectomy from 2012 to 2015 (median age: 68 years), but patients receiving therapy before surgery were excluded. Patient characteristics are summarized in Table I. Although we performed nephrectomy only in 10 stage IV patients with metastasis, this is the standard medical treatment wherever possible. Accordingly, the overall survival (n=45) and recurrence-free survival (n=35) populations differ. In addition, patients underwent FDG-PET/computed tomography (CT) for preoperative staging prior to nephrectomy; SUV_{max} was measured on FDG-PET; and CRP was measured within three weeks before surgery. Several tumor tissue specimens and normal renal parenchymal tissue specimens were harvested from all patients and stored at −80˚C as soon as possible after nephrectomy, as described previously (9, 12). Normal renal parenchymal tissue specimens were obtained from parts of the resected kidneys as far away from the tumor as possible. If the tumor was centrally located, normal parenchymal tissue was attained from the upper or lower pole. The tumor grade and clinical stage were determined by the Fuhrman system and TNM classification, respectively (13, 14). Histopathological examinations of the resected kidneys were performed independently by two pathologists. Patients with abnormalities in putative normal tissue samples through microscopic examination were excluded. This study was conducted in accordance with the Declaration of Helsinki and was approved by the ethics review board of our hospital. Additionally, each patient provided written informed consent.

We typically performed postoperative adjuvant therapy with interferon (IFN)-alpha (3, 5, or 6 million units of natural human IFN-alpha two or three times a week), sorafenib (400 to 800 mg/day), sunitinib (25 to 50 mg/day for 4 weeks, followed by 2 weeks off therapy), or temsirolimus (25 mg/week) if patients had metastatic lesions.

FDG-PET and contrast-enhanced CT. Patients generally received an intravenous injection of FDG (222-333 MBq) at 4.5 MBq/kg after fasting for at least 6 h. Whole-body imaging using a combined FDG-PET/CT scanner (Biograph Sensation 16; Siemens, Erlangen, Germany) and image analysis were performed as described previously (15, 16). The PET and CT scanners covered a region ranging from the brain to the mid-thigh. At 1 h after ^{18}F-FDG injection, CT scanning was conducted and whole-body PET scanning was performed with acquisition for 3 min per bed position using the three-dimensional acquisition mode. Patients underwent contrast-enhanced CT at the same time as PET or within 3 weeks. To acquire the PET/contrast-enhanced CT images, the scans were conducted after CT and PET and subsequent intravenous administration of contrast agent. Additional scans covering only the upper abdomen were performed 40, 75, and 180 s after contrast agent injection, regardless of whether PET/contrast-enhanced CT or contrast-enhanced CT was performed.

Table I. *Patient and tumor characteristics*.

Characteristics	
Patients	45
Age (years)	68 (43-88)
Gender (male/female)	32/13
Follow-up duration (months)	23 (4-46)
Tumors	
Stage (I/II/III/IV)	19/2/14/10
Histological grades (G1/G2/G3/G4)	4/30/9/2
Metastasis (−/+)	35/10

Image analysis. SUV_{max} was determined according to the following formula using Syngo.via software (Siemens Healthcare, Forchheim, Germany):

SUV_{max}=maximum activity in the VOI (MBq/g)/{injected dose (MBq)/body weight (g)}

At the time of the contrast-enhanced CT (2.2 FDG-PET and contrast-enhanced CT), we obtained the enhanced CT images (corticomedullary, nephrographic, and excretory). Thus, the SUV_{max} was measured in reference to these phases. Accordingly, it was not difficult to identify the volume of interest (VOI), even if the lesion had faint FDG (Figure 1A–C). Alternatively, a manual region of interest was drawn in the case of urinary excretion of FDG near the lesion or the presence of an FDG-avid lesion on a spherical VOI (Figure 1D–F) to avoid FDG contamination, for instance in the case of a higher-stage tumor. The PET/CT images were independently reviewed by two physicians: by a certified physician of PET nuclear medicine (HB) as part of a pilot study and by a board-certified nuclear medicine physician (SS) as supervisor.

Real-time reverse transcription-polymerase chain reaction. Total cellular RNA was purified from all 45 sets of tumor and normal renal parenchymal tissue samples with an RNA preparation kit (High Pure RNA Kit; Roche Diagnostic Ltd., Mannheim, Germany) and was used as a template for the synthesis of cDNA. The reaction mixture (100 μl) contained 1 μg of random hexamers and 100 units of MMLV-reverse transcriptase and was incubated at 25˚C for 10 min, 42˚C for 30 min, and then at 99˚C for 5 min. The following primers were used to amplify the indicated genes in tumor tissues after confirmation of their specificity (Takara Bio Ltd., Shiga, Japan): GLUT1, sense, 5'-CTTCCTGCTC ATCAACCGCA-3', antisense, 5'-TGACGATACC GGAGCCAATG-3'; GLUT2, sense, 5'-AGGACTTCTG TGGACCTTAT GTG-3', antisense, 5'-

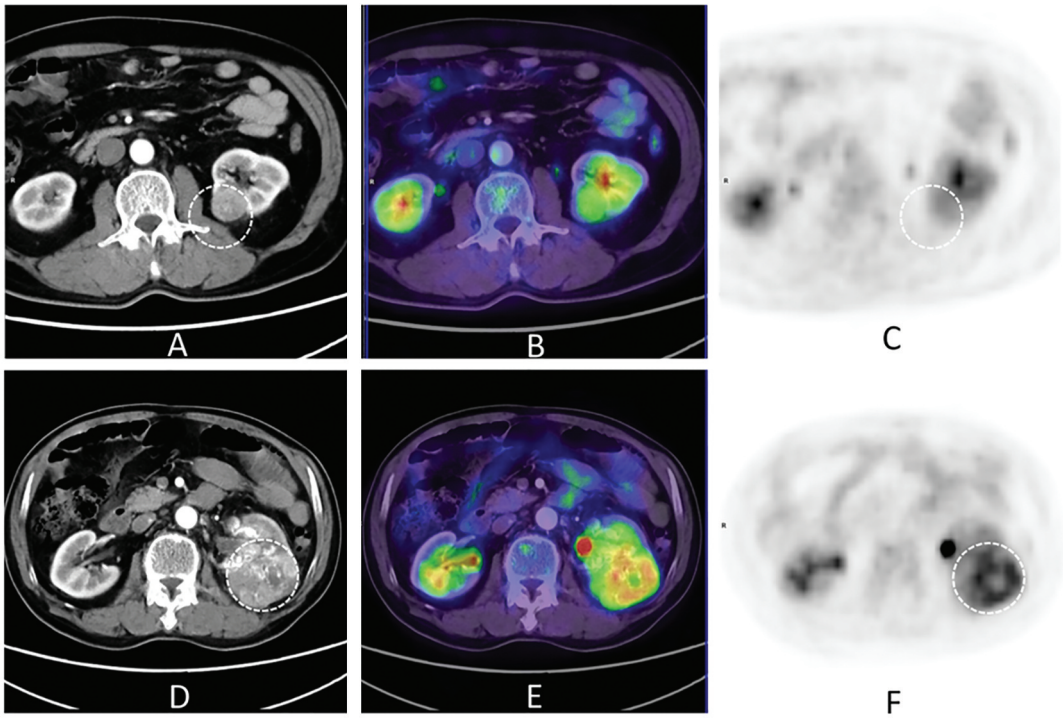

Figure 1. *^{18}F-FDG/CT images of two patients with ccRCC. Axial CT, nephrographic phase (A), fused PET/CT (B), and PET (C) images of a 55-year-old man with ccRCC, G2, pT3aNxM0; SUV_{max} was 3.2 in a spherical VOI. Axial CT, nephrographic phase (D), fused PET/CT (E), and PET (F) images of a 76-year-old man with ccRCC, G3, pT3bNxM0; SUV_{max} was 7.0 in a spherical VOI. A manual region of interest was drawn to avoid urinary excretion of FDG (dashed circle). ccRCC: Clear cell renal cell carcinoma; CT: computed tomography; FDG: ^{18}F-fluorodeoxyglucose; PET: positron emission tomography; SUV: standardized uptake value; VOI: volume-of-interest.*

TTCATGTCA AAAAGCAGGG-3'; SGLT1, sense, 5'-CTCTT CGCC ATTTCTTTCATC-3', antisense, 5'-ATGCACATCC GGAA TGGGT-3'; SGLT2, sense, 5'-AGTGCCTGCT CTGGTTTTGT-3', antisense, 5'-GAGGCTGTGGC TTATGGTGT-3'. Quantitative real-time RT-PCR was performed in a 25-μl reaction mixture containing 20 ng sample cDNA, 100 nM sense primer, 100 nM antisense primer, and 12.5 μl of SYBR Green PCR Master Mix (Applied Biosystems, Foster City, CA, USA). The PCR program included: 45 cycles at 95˚C for 15 s and 60˚C for 1 min using a TP960 Thermal Cycler Dice (Takara Bio Ltd.). A standard curve was generated for each mRNA by five-fold dilution of a control RNA sample, and the expression of each target mRNA was calculated as a ratio to that of 10^3 copies of β-actin (Takara Bio Ltd.) to determine the relative expression level (17, 18). The mean value obtained by the analysis of three samples of resected tissue was calculated as described previously.

Statistical analysis. To analyze the mRNA expression pattern of glucose transporters (GLUT1, GLUT2, SGLT1, SGLT2) and the SUV_{max} of the primary tumors, the 45 patients were classified according to stage I (*n*=19), II (*n*=2), III (*n*=14), and IV (*n*=10)–and grade G1 (*n*=4), G2 (*n*=30), G3 (*n*=9), and G4 (*n*=2). Although we wanted to clarify whether mRNA expression of glucose transporters and SUV_{max} would change with upstaging or upgrading, the numbers of patients for each stage and grade were unbalanced. Therefore, we used the following two sets of categories: I–II (*n*=21) and III–IV (*n*=24), and G1–2 (*n*=34) and G3–4 (*n*=11). We analyzed the mRNA expression of glucose transporters (GLUT1, GLUT2, SGLT1, SGLT2) and SUV_{max} by stage and grade using Student's *t*-test or the Mann-Whitney *U*-test. Kaplan-Meier curves and the log-rank test were used to estimate overall survival and relapse-free survival for groups distributed according to the cutoff values. These curves were based on cutoff points identified using a receiver operating characteristic (ROC) curve and then the patients were divided into two groups. For example, the cutoff point for GLUT1 mRNA was set as 12.3 (copies relative to 10^3 copies of β-actin mRNA) for overall survival. We analyzed several variables (age, sex, stage, grade, metastasis, GLUT1 mRNA, SUV_{max}, and CRP) for overall survival and relapse-free survival by Cox proportional-hazards regression analysis and Kaplan-Meier curves. Spearman's rank correlation coefficient analysis was used to determine the relationship between the expression of GLUT1 mRNA and SUV_{max} values and between CRP values and SUV_{max} values. In all analyses, a *p*-value less than 0.05 was considered statistically significant. Data were analyzed with Microsoft Excel and StatFlex Ver. 6.0 (Artech Ltd., Osaka, Japan).

Results

mRNA expression of glucose transporters. The expression of GLUT1 mRNA was significantly increased in tumor tissue

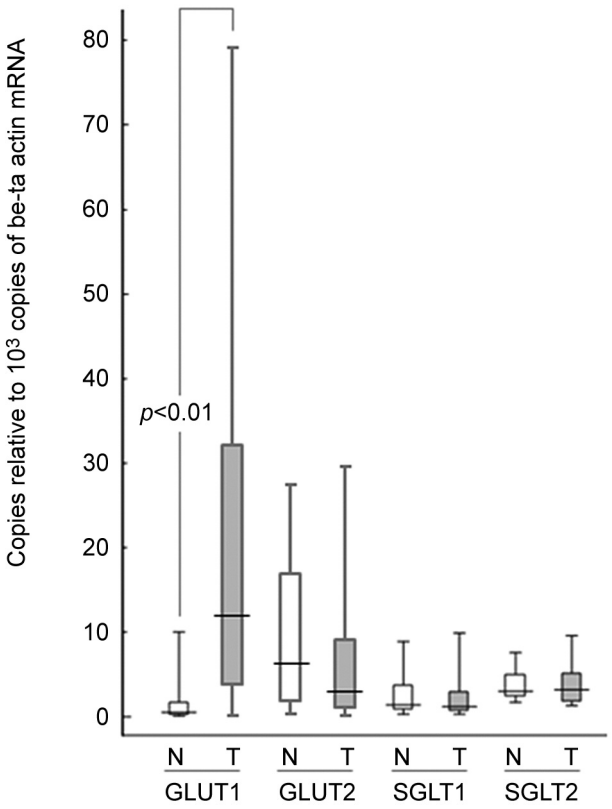

Figure 2. *mRNA expression of the glucose transporters. Statistical significance was evaluated using the Mann-Whitney U-test. N: Normal renal parenchymal tissue; T: tumor tissue. Box plots show median, 10%-90%, 25%, and 75% quartiles.*

(T) (median, 12.7 copies relative to 10^3 copies of β-actin mRNA) compared with normal renal parenchymal tissue (N) (median, 0.5) (Figure 2). However, there was no difference in the expression of other types of glucose transporter mRNA between the tumor tissue and the normal renal parenchymal tissue (Figure 2).

mRNA expression of glucose transporters and SUV_{max} on FDG-PET by stage and grade. Overall median values of the mRNA expression of glucose transporters (GLUT1, GLUT2, SGLT1, SGLT2) and SUV_{max} were (12.7, 3.2, 1.2, 3.2) copies relative to 10^3 copies of β-actin mRNA and 3.9, respectively. Median values of mRNA expression of the glucose transporters GLUT1, GLUT2, SGLT1, and SGLT2 by stage and grade were as follows: Stage I–II, 12.7, 2.1, 0.9, and 2.1, respectively; Stage III–IV, 12.9, 3.6, 1.3, and 3.5, respectively; G1–2, 13.7, 3.0, 1.2, and 3.2, respectively; and G3–4, 8.8, 3.9, 1.2, and 4.6, respectively (Figure 3A-D). Median SUV_{max} values by stage and grade were as follows: Stage I–II, 2.9; Stage III–IV, 4.7; G1–2, 3.6; and G3–4, 4.8 (Figure 3E). Although the mRNA levels of glucose transporters did not correlate with stage or grade (Figure 3A-D), the SUV_{max} of ccRCC positively correlated with both stage and grade (stage: $p<0.01$, Student's *t*-test; grade: $p<0.05$, Mann-Whitney *U*-test; Figure 3E).

Correlation between survival rate and clinicopathological factors. CRP is also indicated as a clinical factor related to tumor progression. Thus, its correlation with overall survival was analyzed ($n=45$). GLUT1 mRNA, SUV_{max}, and CRP were categorized into two groups using the binary variable as a check of clinical validity by ROC analysis and a sensitivity–specificity curve because the results of Cox proportional-hazards regression analyses using continuous variable and binary variable showed no great difference. When CRP of 0.51 (mg/dl), SUV_{max} of 4.6, and a GLUT1 mRNA expression of 12.3 (copies relative to 10^3 copies of β-actin mRNA) were used as cutoff points, the sensitivity, specificity, area under the curve (AUC), and minimum distances from the left upper point (0,1) of the ROC curves were respectively 75.0%, 77.8%, 0.830, and 0.11; 75.0%, 77.8%, 0.830, and 0.11; and 52.8%, 55.6%, 0.556, and 0.42. We also analyzed the correlation with recurrence-free survival in patients who underwent radical nephrectomy ($n=35$), excluding the 10 patients with metastasis who had a nephrectomy, using the following cutoff points: CRP of 0.35 (mg/dl), SUV_{max} of 4.5, and a GLUT1 mRNA expression of 20.5 (copies relative to 10^3 copies of β-actin mRNA). In this case, the sensitivity, specificity, AUC, and minimum distance from the left upper point (0,1) of the ROC curves were respectively 76.7%, 80.0%, 0.900, and 0.06; 90.0%, 90.0%, 0.937, and 0.02; and 70.0%, 66.7%, 0.753, and 0.20.

Kaplan-Meier analysis of overall and recurrence-free survival was performed using the CRP, SUV_{max} and GLUT1 mRNA cutoff points. High CRP and a high SUV_{max} were significantly associated with a poor overall survival and recurrence-free survival rate after surgery ($p<0.01$, Figure 4A, C, and D; $p<0.05$, Figure 4B), unlike GLUT1 mRNA expression ($p=0.30$, Figure 4E; $p=0.05$, Figure 4F). We examined the statistical association of overall survival with age, sex, stage, grade, metastasis, CRP, GLUT1 mRNA, and SUV_{max}. Metastasis, CRP, and SUV_{max} were individually confirmed to be significant factors in univariate regression analyses (Table II). These factors were correlated with each other according to Fisher's exact test and the χ^2-test (Table III).

Correlation of SUV_{max} with GLUT1 mRNA and CRP. There was no correlation between SUV_{max} and GLUT1 mRNA expression (Figure 5A), but there was a correlation between SUV_{max} and CRP (Spearman's rank correlation r=0.457, $p<0.01$; Figure 5B). Furthermore, by considering the result shown in Figure 5B, it was confirmed that there was

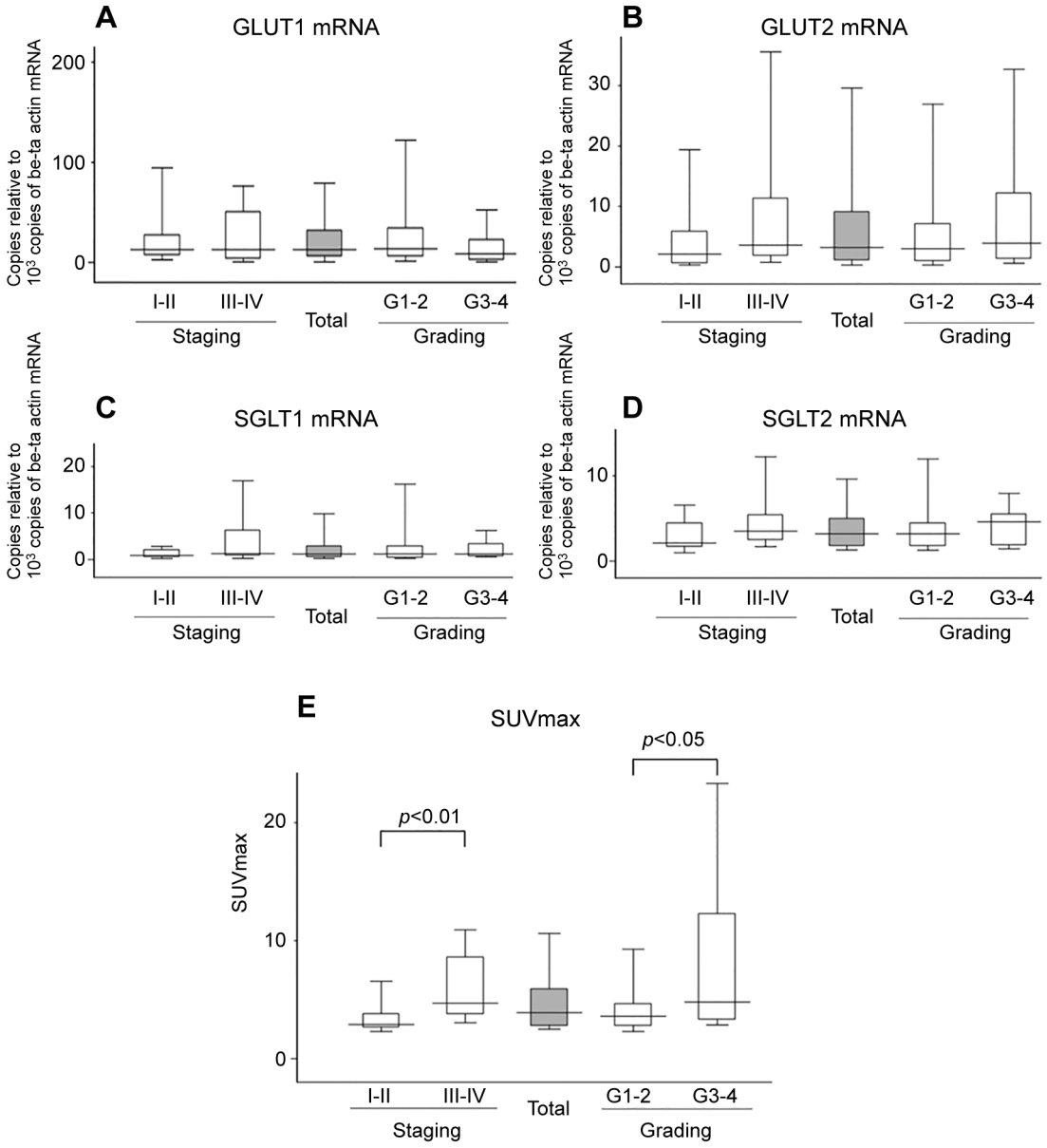

Figure 3. *Correlation of the mRNA expression levels of glucose transporters (GLUT1, GLUT2, SGLT1, SGLT2) (A-D) and SUV_{max} values (E) with both staging and grading. A Kruskal-Wallis test was used for staging, and a Mann-Whitney U-test was used for grading. In (E), the two-sample t-test was used to compare groups I-II vs. III-IV. The Mann-Whitney test was used to compare groups G1-2 vs. G3-4. GLUT: Glucose transporter; SUV: standardized uptake value.*

multicollinearity between SUV_{max} and CRP. Thus, multivariate regression analysis of metastasis, SUV_{max}, and GLUT1 mRNA was performed (Table II). However, no factors were independently associated with prognosis. According to the analysis of recurrence-free survival, CRP was confirmed to be a significant factor in univariate regression analysis, and SUV_{max} could not be analyzed due to the close relationship between the higher SUV_{max} uptake group and the recurrence group (Table IV).

Discussion

By comparing primary ccRCC with normal renal parenchymal tissues, we aimed to examine how the mRNA expression of glucose transporters (GLUT1, GLUT2, SGLT1, and SGLT2) changed and whether these glucose transporters related to FDG accumulation and prognosis. We showed that GLUT1 mRNA was over-expressed, although no significant change was found for GLUT2, SGLT1, and

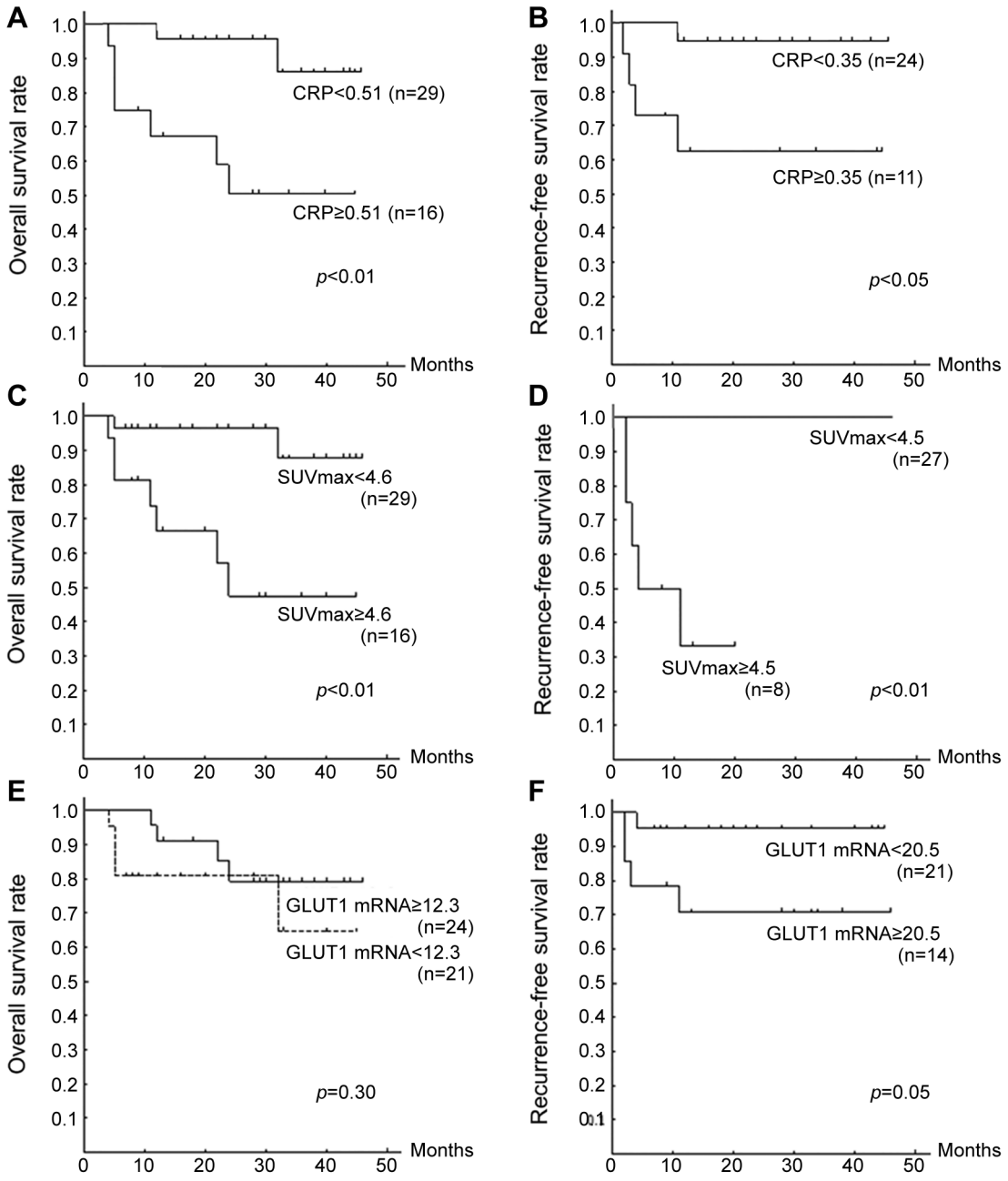

Figure 4. *Overall survival curves (n=45) and recurrence-free survival curves (n=35). (A) CRP: lower group <0.51 (mg/dl), higher group ≥0.51 (mg/dl), (B) CRP: lower group <0.35, higher group ≥0.35 [same as (A)], (C) SUV_{max}: lower uptake group <4.6, higher uptake group ≥4.6. (D) SUV_{max}: lower uptake group <4.5 [same as (C)]. (E) GLUT1 mRNA: higher expression group ≥12.3, lower expression group <12.3, higher uptake group ≥12.3. (F) GLUT1 mRNA: higher expression group ≥20.5 [same as (E)]. CRP: C-reactive protein; GLUT: glucose transporter; SUV: standardized uptake value.*

SGLT2. These findings resemble those of a study by Chan *et al*. (3) and the results of staining with GLUT1 for malignant thymic epithelial tumors (5). The lesion expression patterns from the above analyses would probably result in an upregulated glycometabolism due to GLUT1 mRNA over-expression and tumor progression. However, there was no relationship between GLUT1 mRNA and stage, grade, or survival in our study. Thus, specific glycometabolism-related glucose transporters could not be linked to ccRCC.

Table II. *Univariate and multivariate regression analyses using the Cox proportional-hazards model for prediction of overall survival (n=45).*

		Univariate analysis		Multivariate analysis	
Variable	Case number	*p*-Value	Relative risk (95%CI)	*p*-Value	Relative risk (95%CI)
Age ≥68 (years)	22	0.056	0.13 (0.02-1.05)		
Gender: male	32	0.688	1.38 (0.29-6.66)		
Stage: high stage (III, IV)	24	0.059	7.44 (0.93-59.66)		
Grade: high grade (G3-4)	11	0.081	3.24 (0.86-12.23)		
Metastasis at surgery	10	<0.01	7.91 (1.98-31.66)	0.154	3.49 (0.63-19.48)
CRP ≥0.51 (mg/dl)	16	<0.05	7.34 (1.52-35.41)		
SUVmax ≥4.6	16	<0.05	7.83 (1.62-37.91)	0.146	3.94 (0.62-25.03)
GLUT1 mRNA ≥12.3 (copies relative to 10^3 copies of β-actin mRNA)	24	0.307	0.50 (0.13-11.89)	0.750	0.79 (0.19-3.32)

Univariate and multivariate regression analyses of overall survival were performed using the Cox proportional-hazards model. The cutoff points: When CRP of 0.51 (mg/dl), SUV_{max} of 4.6, and a GLUT1 mRNA expression of 12.3 (copies relative to 10^3 copies of β-actin mRNA) were used as cutoff points, the sensitivity, specificity, area under the curve (AUC), and minimum distances from the left upper point (0,1) of the ROC curves were respectively 75.0%, 77.8%, 0.830, and 0.11; 75.0%, 77.8%, 0.830, and 0.11; and 52.8%, 55.6%, 0.556, and 0.42. GLUT: Glucose transporter; CRP: C-reactive protein; SUV: standardized uptake value.

Based on the analysis of FDG accumulation, FDG uptake increased with both upstaging and upgrading. Thus, it can be suggested that an increased FDG uptake in primary ccRCC is related to poor prognosis.

In the kidney, GLUT1, GLUT2, SGLT1, and SGLT2, which belong to distinct glucose transporter families, play roles in facilitative and secondary active transport at renal proximal tubular epithelial cells. Most ccRCCs arise from these cells. In ccRCCs, von Hippel-Lindau (VHL) tumor suppressor protein becomes inactivated by mutation (>50%) or methylation (5%-10%) (19-21). This leads to upregulation of hypoxia-inducible factor (HIF)-1, which is normally induced under hypoxic conditions, followed by enhanced transcription of several targets, such as GLUT1 and vascular endothelial growth factor (22).

In this study, we showed increased FDG uptake and GLUT1 mRNA over-expression in ccRCCs. Our results appear to be concordant with those of studies examining glucose metabolism in RCC (3, 23). Although many studies of FDG uptake in other malignancies have been published (5, 24, 25), none have examined the relationship between FDG uptake, GLUT1, and RCC. The following are possible reasons for this gap. One is the rather faint FDG uptake in many RCCs, which is especially common in early stages. As described above, our data showed that the median SUV_{max} value in ccRCC stage I–II was just 2.9. These results could indicate a technical limitation to the accurate measurement of the accumulation because of a lower contrast between the RCCs and the surrounding renal tissue/adjacent urinary tract; these regions have faint-to-strong FDG uptake physiologically. Miyakita *et al*. (26) calculated the SUV of kidney tumors in 10 patients, obtaining a value of 2.42±1.40, and Bachor *et al*. (27) reported that RCC was overlooked preoperatively in 6 of 26 patients with histologically proven RCC because of a false negative diagnosis on PET. Miyakita *et al*. (26) also suggested that RCC cells themselves have a low potential for glucose metabolism and that FDG accumulation is decreased, even though GLUT1 is over-expressed in many RCCs. However, Steinberg *et al*. (28) and Schmoll *et al*. (29) showed that glucose 6-phosphatase was strongly reduced in RCCs compared with control kidney tissue of the same patient. In addition, hexokinase (HK) 2, which is an HK isozyme and a key molecule for glycolysis in cancer cells (30), is over-expressed in RCC tissues (23). Considering the abovementioned reports of increased glucose metabolism in RCCs (23, 28, 29), we calculated the SUV_{max} of lesions carefully, even if they only showed faint FDG accumulation. Accordingly, we were able to determine the relationship between FDG accumulation in the lesions and parameters such as stage, histological grade, and prognosis. Thus, we hypothesize that these are the reasons for the paucity of reports regarding FDG accumulation and metabolism in RCCs.

Table III. *Factor correlation analysis (metastasis, CRP and SUV_{max}).*

Parameters	Metastasis	CRP≥0.51 (mg/dl)	SUV_{max}≥4.6
Metastasis at surgery (metastasis)			
CRP ≥0.51 (mg/dl)	<0.05		
SUV_{max}≥4.6	<0.01	*<0.001	

The *p*-value of each correlation was calculated using Fisher's exact test or the *χ^2-test. CRP: C-reactive protein; SUV: standardized uptake value.

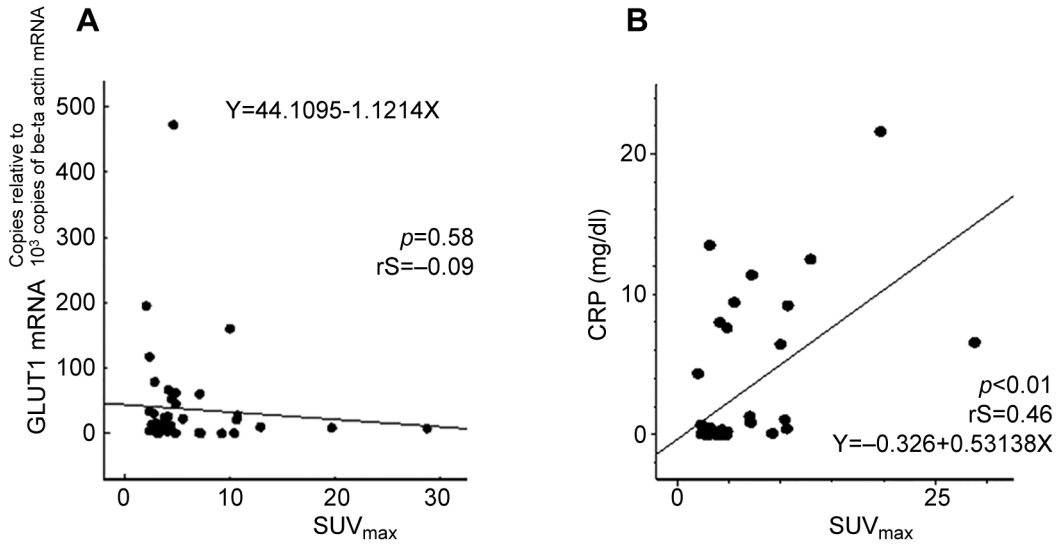

Figure 5. *Spearman's rank correlation of SUV_{max} values with GLUT1mRNA levels (A) and CRP values (B). GLUT: Glucose transporter; SUV: standardized uptake value; CRP: C-reactive protein.*

Here, we also examined FDG accumulation and glucose transporter mRNA. We initially hypothesized that the abnormal FDG uptake would arise from GLUT1 mRNA over-expression. However, there was no correlation between FDG and GLUT1 mRNA. Thus, we postulate that the abnormal FDG uptake might be caused by other catalyzing substances besides GLUT1, but we did not explore alternative molecular pathways of FDG uptake, for example, glucose 6-phosphatase and HK.

We also showed that SUV_{max} on PET-CT was related to metastasis and CRP by the chi-square test. Kaplan-Meier curves showed that SUV_{max} and CRP were significantly associated with overall and recurrence-free survival rates. In particular, the higher SUV_{max} group was strongly associated with the recurrence group, meaning that multivariate regression analysis could not be performed due to the close relationship between these two groups. Spearman's correlation between SUV_{max} and CRP showed a strong correlation. Thus, both SUV_{max} and CRP could be prognostic factors.

Thus, we propose the following: in many ccRCCs, the VHL pathway is inactivated and HIF is upregulated, followed by over-expression of GLUT1 and HK2 (3, 23). This mechanism, which results in an increase in the glycolytic system, could be reflected in SUV_{max}. Accordingly, we predict that high SUV_{max} and CRP are related to poor prognosis, even though SUV_{max} is generally low in ccRCC.

Because our findings were limited to a portion of the glycolytic system, the exploration of other enzymes involved in the glycolytic system and FDG accumulation is required. In future work, we hope to clarify the mechanisms underlying the progression of ccRCC. A high SUV_{max} and GLUT1 mRNA over-expression were observed in primary ccRCC. SUV_{max} increased with upstaging and upgrading, unlike GLUT1 mRNA. Moreover, there was no correlation between SUV_{max} and GLUT1 mRNA, indicating the possible involvement of other metabolic mechanisms in ccRCC.

Table IV. *Univariate regression analysis of recurrence-free survival using the Cox proportional-hazards model (n=35).*

Variable	Case number	Univariate analysis	
		p-Value	Relative risk (95%CI)
Age>68 (years)	20	0.116	0.17 (0.02-1.55)
Stage: high stage (III)	14	0.088	6.74 (0.75-60.37)
Grade: high grade (G3-4)	05	0.147	3.76 (0.63-22.52)
CRP≥0.35 (mg/dl)	11	<0.05	9.42 (1.05-64.38)
SUV_{max}≥4.5	08	*	
GLUT1 mRNA≥20.5 (copies relative to 10^3 copies of β-actin mRNA)	14	0.094	6.51 (0.73-58.38)

The cutoff points were CRP of 0.35 (mg/dl), SUV_{max} of 4.5, and a GLUT1 mRNA expression of 20.5 (copies relative to 10^3 copies of β-actin mRNA). The sensitivity, specificity, AUC, and minimum distance from the left upper point (0,1) of the ROC curves were respectively 76.7%, 80.0%, 0.900, and 0.06; 90.0%, 90.0%, 0.937, and 0.02; and 70.0%, 66.7%, 0.753, and 0.20. *Could not be analyzed due to the close relationship between the higher SUV_{max} uptake group and the recurrence group. GLUT: Glucose transporter; CRP: C-reactive protein; SUV: standardized uptake value.

Conflicts of Interest

The Authors have no conflicts of interest directly relevant to the content of this article.

Authors' Contributions

Concept development and manuscript preparation (HB, SS, YK, NA, TK), Data generation (HB, SS, YK, AN, MY, TK), Experimental design (HB, SS, MK, KH), Data analysis (HB, SS). All Authors cooperated in the internal review of the manuscript prior to submission.

Acknowledgements

The Authors thank Hitomi Sakuraoka, Mai Takahashi, Kyoko Arai, Masaya Seki and Kazumi Akimoto for their skillful technical assistance. This research received no specific grant from any funding agency in the public, commercial, or not-for-profit sectors.

References

1 Thorens B and Mueckler M: Glucose transporters in the 21st Century. Am J Physiol Endocrinol Metab *298(2)*: E141-E145, 2010. PMID: 20009031. DOI: 10.1152/ajpendo.00712.2009

2 Gyimesi G, Pujol-Giménez J, Kanai Y and Hediger MA: Sodium-coupled glucose transport, the SLC5 family, and therapeutically relevant inhibitors: from molecular discovery to clinical application. Pflugers Arch *472(9)*: 1177-1206, 2020. PMID: 32767111. DOI: 10.1007/s00424-020-02433-x

3 Chan DA, Sutphin PD, Nguyen P, Turcotte S, Lai EW, Banh A, Reynolds GE, Chi JT, Wu J, Solow-Cordero DE, Bonnet M, Flanagan JU, Bouley DM, Graves EE, Denny WA, Hay MP and Giaccia AJ: Targeting GLUT1 and the Warburg effect in renal cell carcinoma by chemical synthetic lethality. Sci Transl Med *3(94)*: 94ra70, 2011. PMID: 21813754. DOI: 10.1126/scitranslmed.3002394

4 Chen CH, Wang BW, Hsiao YC, Wu CY, Cheng FJ, Hsia TC, Chen CY, Wang Y, Weihua Z, Chou RH, Tang CH, Chen YJ, Wei YL, Hsu JL, Tu CY, Hung MC and Huang WC: PKCδ-mediated SGLT1 upregulation confers the acquired resistance of NSCLC to EGFR TKIs. Oncogene *40(29)*: 4796-4808, 2021. PMID: 34155348. DOI: 10.1038/s41388-021-01889-0

5 Nakajo M, Kajiya Y, Tani A, Yoneda S, Shirahama H, Higashi M and Nakajo M: ^{18}FDG PET for grading malignancy in thymic epithelial tumors: significant differences in ^{18}FDG uptake and expression of glucose transporter-1 and hexokinase II between low and high-risk tumors: preliminary study. Eur J Radiol *81(1)*: 146-151, 2012. PMID: 20810231. DOI: 10.1016/j.ejrad.2010.08.010

6 Kobayashi M, Uematsu T, Tokura Y, Takei K, Sakamoto K, Narimatsu T, Nukui A and Kamai T: Immunohistochemical expressionof sodium-dependent glucose transporter-2 (SGLT-2) in clear cell renal carcinoma: possible prognostic implications. Int Braz J Urol *45(1)*: 169-178, 2019. PMID: 30521176. DOI: 10.1590/S1677-5538.IBJU.2018.0271

7 Verhoeff SR, van Es SC, Boon E, van Helden E, Angus L, Elias SG, Oosting SF, Aarntzen EH, Brouwers AH, Kwee TC, Heskamp S, Hoekstra OS, Verheul H, van der Veldt AAM, de Vries EGE, Boerman OC, van der Graaf WTA, Oyen WJG and van Herpen CML: Lesion detection by [^{89}Zr]Zr-DFO-girentuximab and [^{18}F]FDG-PET/CT in patients with newly diagnosed metastatic renal cell carcinoma. Eur J Nucl Med Mol Imaging *46(9)*: 1931-1939, 2019. PMID: 31172212. DOI: 10.1007/s00259-019-04358-9

8 Nakaigawa N, Kondo K, Ueno D, Namura K, Makiyama K, Kobayashi K, Shioi K, Ikeda I, Kishida T, Kaneta T, Minamimoto R, Tateishi U, Inoue T and Yao M: The acceleration of glucose accumulation in renal cell carcinoma assessed by FDG PET/CT demonstrated acquisition of resistance to tyrosine kinase inhibitor therapy. BMC Cancer *17(1)*: 39, 2017. PMID: 28068944. DOI: 10.1186/s12885-016-3044-0

9 Mizuno T, Kamai T, Abe H, Sakamoto S, Kitajima K, Nishihara D, Yuki H, Kambara T, Betsunoh H, Yashi M, Fukabori Y, Kaji Y and Yoshida K: Clinically significant association between the maximum standardized uptake value on 18F-FDG PET and expression of phosphorylated Akt and S6 kinase for prediction of the biological characteristics of renal cell cancer. BMC Cancer *15*: 1097, 2015. PMID: 25784113. DOI: 10.1186/s12885-015-1097-0

10 Nakajima R, Matsuo Y, Kondo T, Abe K and Sakai S: Prognostic value of metabolic tumor volume and total lesion glycolysis on preoperative 18F-FDG PET/CT in patients with renal cell carcinoma. Clin Nucl Med *42(4)*: e177-e182, 2017. PMID: 28134692. DOI: 10.1097/RLU.0000000000001552

11 Saito K, Tatokoro M, Fujii Y, Iimura Y, Koga F, Kawakami S and Kihara K: Impact of C-reactive protein kinetics on survival of patients with metastatic renal cell carcinoma. Eur Urol *55(5)*: 1145-1153, 2009. PMID: 18930583. DOI: 10.1016/j.eururo.2008.10.012

12 Betsunoh H, Fukuda T, Anzai N, Nishihara D, Mizuno T, Yuki H, Masuda A, Yamaguchi Y, Abe H, Yashi M, Fukabori Y, Yoshida K and Kamai T: Increased expression of system large amino acid transporter (LAT)-1 mRNA is associated with invasive potential and unfavorable prognosis of human clear cell renal cell carcinoma. BMC Cancer *13*: 509, 2013. PMID: 24168110. DOI: 10.1186/1471-2407-13-509

13 Fuhrman SA, Lasky LC and Limas C: Prognostic significance of morphologic parameters in renal cell carcinoma. Am J Surg Pathol *6(7)*: 655-663, 1982. PMID: 7180965. DOI: 10.1097/00000478-198210000-00007

14 Sobin LH, Gospodarowicz MK and Wittekind CH: International union against cancer. UICC. In: TNM Classification of Malignant Tumors. 7th ed. Sobin LH, Gospodarowicz MK, Wittekind C (eds.). New York, Wiley-Blackwell, pp. 255-257, 2009.

15 Kitajima K, Murakami K, Kaji Y, Sakamoto S and Sugimura K: Established, emerging and future applications of FDG-PET/CT in the uterine cancer. Clin Radiol *66(4)*: 297-307, 2011. PMID: 21356392. DOI: 10.1016/j.crad.2010.07.012

16 Kitajima K, Murakami K, Yamasaki E, Fukasawa I, Inaba N, Kaji Y and Sugimura K: Accuracy of 18F-FDG PET/CT in detecting pelvic and paraaortic lymph node metastasis in patients with endometrial cancer. AJR Am J Roentgenol *190(6)*: 1652-1658, 2008. PMID: 18492920. DOI: 10.2214/AJR.07.3372

17 Betsunoh H, Mukai S, Akiyama Y, Fukushima T, Minamiguchi N, Hasui Y, Osada Y and Kataoka H: Clinical relevance of hepsin and hepatocyte growth factor activator inhibitor type 2 expression in renal cell carcinoma. Cancer Sci *98(4)*: 491-498, 2007. PMID: 17309599. DOI: 10.1111/j.1349-7006.2007.00412.x

18 Kamai T, Yanai Y, Arai K, Abe H, Yamanishi T, Kurimoto M and Yoshida K: Increased interferon alpha receptor 2 mRNA levels is associated with renal cell carcinoma metastasis. BMC Cancer *7*: 159, 2007. PMID: 17697365. DOI: 10.1186/1471-2407-7-159

19 Nickerson ML, Jaeger E, Shi Y, Durocher JA, Mahurkar S, Zaridze D, Matveev V, Janout V, Kollarova H, Bencko V, Navratilova M, Szeszenia-Dabrowska N, Mates D, Mukeria A, Holcatova I, Schmidt LS, Toro JR, Karami S, Hung R, Gerard GF, Linehan WM, Merino M, Zbar B, Boffetta P, Brennan P, Rothman N, Chow WH, Waldman FM and Moore LE: Improved identification of von Hippel-Lindau gene alterations in clear cell renal tumors. Clin Cancer Res *14(15)*: 4726-4734, 2008. PMID: 18676741. DOI: 10.1158/1078-0432.CCR-07-4921

20 Gnarra JR, Tory K, Weng Y, Schmidt L, Wei MH, Li H, Latif F, Liu S, Chen F and Duh FM: Mutations of the VHL tumour suppressor gene in renal carcinoma. Nat Genet *7(1)*: 85-90, 1994. PMID: 7915601. DOI: 10.1038/ng0594-85

21 Herman JG, Latif F, Weng Y, Lerman MI, Zbar B, Liu S, Samid D, Duan DS, Gnarra JR and Linehan WM: Silencing of the VHL tumor-suppressor gene by DNA methylation in renal carcinoma. Proc Natl Acad Sci U.S.A. *91(21)*: 9700-9704, 1994. PMID: 7937876. DOI: 10.1073/pnas.91.21.9700

22 Isaacs JS, Jung YJ, Mole DR, Lee S, Torres-Cabala C, Chung YL, Merino M, Trepel J, Zbar B, Toro J, Ratcliffe PJ, Linehan WM and Neckers L: HIF overexpression correlates with biallelic loss of fumarate hydratase in renal cancer: novel role of fumarate in regulation of HIF stability. Cancer Cell *8(2)*: 143-153, 2005. PMID: 16098467. DOI: 10.1016/j.ccr.2005.06.017

23 Yoshino H, Enokida H, Itesako T, Kojima S, Kinoshita T, Tatarano S, Chiyomaru T, Nakagawa M and Seki N: Tumor-suppressive microRNA-143/145 cluster targets hexokinase-2 in renal cell carcinoma. Cancer Sci *104(12)*: 1567-1574, 2013. PMID: 24033605. DOI: 10.1111/cas.12280

24 Izuishi K, Yamamoto Y, Mori H, Kameyama R, Fujihara S, Masaki T and Suzuki Y: Molecular mechanisms of [18F]fluorodeoxyglucose accumulation in liver cancer. Oncol Rep *31(2)*: 701-706, 2014. PMID: 24297035. DOI: 10.3892/or.2013.2886

25 Mamede M, Higashi T, Kitaichi M, Ishizu K, Ishimori T, Nakamoto Y, Yanagihara K, Li M, Tanaka F, Wada H, Manabe T and Saga T: [18F]FDG uptake and PCNA, Glut-1, and Hexokinase-II expressions in cancers and inflammatory lesions of the lung. Neoplasia *7(4)*: 369-379, 2005. PMID: 15967114. DOI: 10.1593/neo.04577

26 Miyakita H, Tokunaga M, Onda H, Usui Y, Kinoshita H, Kawamura N and Yasuda S: Significance of 18F-fluorodeoxyglucose positron emission tomography (FDG-PET) for detection of renal cell carcinoma and immunohistochemical glucose transporter 1 (GLUT-1) expression in the cancer. Int J Urol *9(1)*: 15-18, 2002. PMID: 11972644. DOI: 10.1046/j.1442-2042.2002.00416.x

27 Bachor R, Kotzerke J, Gottfried HW, Brändle E, Reske SN and Hautmann R: Positron emission tomography in diagnosis of renal cell carcinoma. Urologe A *35(2)*: 146-150, 1996. PMID: 8650849.

28 Steinberg P, Störkel S, Oesch F and Thoenes W: Carbohydrate metabolism in human renal clear cell carcinomas. Lab Invest *67(4)*: 506-511, 1992. PMID: 1434530.

29 Schmoll D, Balabanov S, Schwarck D, Burchell A, Kleist B, Zimmermann U and Walther R: Differential expression of the subunits of the glucose-6-phosphatase system in the clear cell type of human renal cell carcinoma – no evidence for an overexpression of protein kinase B. Cancer Lett *167(1)*: 85-90, 2001. PMID: 11323102. DOI: 10.1016/s0304-3835(01)00465-7

30 Mathupala SP, Ko YH and Pedersen PL: Hexokinase II: cancer's double-edged sword acting as both facilitator and gatekeeper of malignancy when bound to mitochondria. Oncogene *25(34)*: 4777-4786, 2006. PMID: 16892090. DOI: 10.1038/sj.onc.1209603

Received July 8, 2021
Revised August 10, 2021
Accepted August 11, 2021